

# High-resolution terahertz spectrum of CH<sub>2</sub> — Low *J* rotational transitions near 2 THz<sup>1</sup>

S. Brünken, E.A. Michael, F. Lewen, Th. Giesen, H. Ozeki, G. Winnewisser, P. Jensen, and E. Herbst

**Abstract:** The methylene radical (CH<sub>2</sub>) was very important to Gerhard Herzberg. We have carried out high-resolution spectroscopic measurements on two energetically low-lying, pure rotational transitions of methylene in its ground vibrational–electronic state at frequencies near 2 THz. One of the transitions — the  $N_{KaKc} = 2_{11} \leftarrow 2_{02}$  multiplet — belongs to *ortho*-CH<sub>2</sub> and is centered at 1.954 THz. The other rotational transition — the  $N_{KaKc} = 1_{10} \leftarrow 1_{01}$  multiplet — belongs to *para*-CH<sub>2</sub> and is centered at 1.915 THz. Since the ground electronic state of methylene has <sup>3</sup>B<sub>1</sub> symmetry, the rotational transitions are split into three fine-structure components, while the *ortho* transitions are split additionally by hyperfine structure. In total, we have measured 29 new lines, six for the *para* transition and the remainder for the *ortho* transition. The newly measured lines can be added to high-resolution spectral data obtained by ourselves and others at lower frequencies. Progress towards a global fit is discussed.

*Key words:* spectroscopy, THz frequencies, radicals, methylene, interstellar medium.

**Résumé :** Le radical méthylène (CH<sub>2</sub>) a été très important pour Gerhard Herzberg. On a effectué des mesures spectroscopiques à haute résolution sur deux transitions de rotation pure, de basses énergies, du méthylène dans l'état électronique–vibrationnel fondamental, à des fréquences proches de 2 THz. L'une des transitions, celle du multiplet  $N_{KaKc} = 2_{11} \leftarrow 2_{02}$ , appartient au CH<sub>2</sub> *ortho* et elle est centrée à 1,954 THz. L'autre transition rotationnelle, celle du multiplet  $N_{KaKc} = 1_{10} \leftarrow 1_{01}$ , appartient au CH<sub>2</sub> *para* et elle est centrée à 1,915 THz. Puisque l'état électronique fondamental du méthylène est de symétrie <sup>3</sup>B<sub>1</sub>, les transitions rotationnelles sont dédoublées en une structure de trois composantes alors que les transitions *ortho* subissent un dédoublement additionnel par une structure hyperfine. Au total, on a mesuré 29 nouvelles raies, six pour la transition *para* et le reste pour la transition *ortho*. On peut ajouter les raies nouvellement mesurées aux données spectrales obtenues par nos soins et à celles obtenues à des fréquences plus faibles par d'autres. On discute des progrès réalisés dans le développement d'un ajustement global.

*Mots clés :* spectroscopie, fréquences THz, radicaux, méthylène, système interstellaire.

[Traduit par la Rédaction]

## Introduction

### Gerhard Herzberg and methylene

The methylene radical (CH<sub>2</sub>) was of great interest to Gerhard Herzberg (1). The initial attempt to discover this species in the laboratory dates back to the year 1942, when Gerhard Herzberg was first trying to study the electronic spectra of free radicals. By discharging methane (CH<sub>4</sub>), Herzberg thought very early on that he had produced the

spectrum of the free radical CH<sub>2</sub>. But in reality, it took many more years than anticipated before the methylene radical was finally discovered. This seminal event took place “seventeen years after Herzberg’s first involvement with CH<sub>2</sub>; proving his persistence and determination to finally solve this puzzle” (1). The discovery took place when Herzberg and Shoosmith (2) located a prominent new feature on their photographic plate in the extreme UV region at 1415 Å. Although Herzberg initially thought that methylene was linear in its ground state, detailed analyses of the spectra led eventually to the assignment of the ground state as one of <sup>3</sup>B<sub>1</sub> symmetry with a nonlinear symmetrical structure, C–H bond distances of 1.071 Å, and an H–C–H angle of 140° (3), settling another long-standing problem. According to Herzberg’s Nobel lecture (4), he had spent more than 20 years determining the nature of the electronic states of this difficult radical.

Gerhard Herzberg was so interested in improving our knowledge of methylene that after his successful assignment of the ground electronic state, he soon thought in terms of studying its rotational spectrum. One of us (G. Winnewisser) was a postdoctoral associate at NRC in Ottawa during the years 1968–1970. He had recently constructed a submillimeter-wave spectrometer for the NRC, so Herzberg asked him to attempt to study methylene. The request was then regretfully de-

Received 30 December 2003. Published on the NRC Research Press Web site at <http://canjchem.nrc.ca> on 26 May 2004.

**S. Brünken, E.A. Michael, F. Lewen, G. Winnewisser, and Th. Giesen.** Physikalisches Institut, Universität zu Köln, Zùlpicher Str. 77, D-50937 Köln, Germany.

**H. Ozeki.** ISS Science Project Office, Japan Aerospace Exploration Agency, Tsukuba, 305-8505, Japan.

**P. Jensen.** Fachgruppe Chemie, Bergische Universität Wuppertal, D-42097 Wuppertal, Germany.

**E. Herbst.**<sup>2</sup> Departments of Physics, Chemistry, and Astronomy, The Ohio State University, Columbus, OH 43210.

<sup>1</sup>This article is part of a Special Issue dedicated to the memory of Professor Gerhard Herzberg.

<sup>2</sup>Corresponding author (e-mail: [herbst@mps.ohio-state.edu](mailto:herbst@mps.ohio-state.edu)).

clined; Herzberg's requests for CH<sub>2</sub> microwave data were, just as the man himself, simply 25 years ahead of the time.

More than 10 years after Herzberg's success, work on methylene began anew. In the early eighties, there was a strong push within the spectroscopy group at NRC, led by P.R. Bunker and A.R.W. McKellar, and with the strong involvement of T.J. Sears and P. Jensen, to detect the IR spectrum of CH<sub>2</sub>. The goal was to find vibration-rotation transitions of the  $\nu_2$  bending vibration of the radical in its <sup>3</sup>B<sub>1</sub> electronic ground state. After much effort, the  $\nu_2$  bending vibration was finally detected using laser magnetic resonance (LMR) techniques in the wavenumber range 880–940 cm<sup>-1</sup> (5). The present best numerical value for the bending frequency of CH<sub>2</sub> is 963 cm<sup>-1</sup> (6). Although the symmetric and antisymmetric stretching vibrations (the  $\nu_1$  and  $\nu_3$  modes) remain undetected, reasonable estimates for these frequencies (2992 and 3213 cm<sup>-1</sup>) are available from calculations based on the MORBID approach (6). Another push at NRC involved using the very sensitive LMR technique to study the rotational spectrum of methylene. Eventually, LMR was used to study the rotational spectrum through 6 THz in frequency (7, 8). In addition, diode laser spectroscopy was used to study five rotational transitions involving  $K_a = 4 \leftarrow 3$  at frequencies near 12 THz (9).

Although the LMR technique possesses great frequency agility for the study of rotational spectra, it does not approach the accuracy of millimetre- and submillimetre-wave methods. But, the field-free rotational spectrum of methylene, a near-prolate asymmetric top with a dipole moment of 0.57 D along the intermediate *b* axis (10), has proved a difficult one to measure because of its wide-open structure due to the lightness of the radical, because of large amplitude motions, and because of both fine and hyperfine splittings. The wide spacings between most pairs of rotational levels mean that much of the rotational spectrum lies in the THz region.

The rotational energy levels of methylene are characterized by the quantum number *N* and the pseudo-quantum numbers  $K_a$  and  $K_c$ . The quantum number *N* refers to rigid-body angular momentum of the asymmetric top and replaces the normal symbol *J*, which is used here for the total nonnuclear angular momentum (rigid-body + electronic spin). The pseudo-quantum numbers  $K_a$  and  $K_c$  refer to the rigid-body angular momentum projection on the symmetry axes of the limiting prolate and oblate symmetric tops, respectively. Since the electronic spin quantum number *S* = 1 for CH<sub>2</sub> in its <sup>3</sup>B<sub>1</sub> ground state, the values of *J* are *N*, *N* + 1, *N* - 1 for *N* > 0. Energy levels of the same *N* and differing *J* are split by fine-structure effects. In addition to the fine structure, *N*,*J* levels of *ortho*-CH<sub>2</sub>, which possesses a total hydrogenic nuclear spin *I<sub>H</sub>* of unity, are split by hyperfine effects into energy levels characterized by the total angular momentum quantum number  $F = J, J + 1, J - 1$  for *J* > 0. On the other hand, the *N*,*J* levels of *para*-CH<sub>2</sub>, where *I<sub>H</sub>* = 0, are not split further by hyperfine effects. Given the splittings and the dipolar selection rules ( $\Delta N = 0, \pm 1$ ;  $\Delta J = 0, \pm 1$ ,  $\Delta F = 0, \pm 1$ ) rotational transitions of *ortho*- and *para*-CH<sub>2</sub> occur in multiplets of lines, with the components for the *ortho* form much more numerous and closely spaced. For *ortho*-CH<sub>2</sub>, only rotational levels characterized by an even value for the sum  $K_a + K_c$  are allowed (e.g., 4<sub>04</sub> and 3<sub>13</sub>), whereas for

*para*-CH<sub>2</sub> levels, the sum must be odd. The allowed changes in these two pseudo-quantum numbers for *b*-type transitions are  $\Delta K_a = \pm 1, \pm 3, \dots$ ,  $\Delta K_c = \pm 1, \pm 3, \dots$

Lovas et al. (11) were the first to study the high-resolution rotational spectrum; they measured the multiplet of lines in the 68–71 GHz range belonging to the rather high-lying  $N_{K_a K_c} = 4_{04} \leftarrow 3_{13}$  transition of *ortho*-CH<sub>2</sub>. These lines were later used to detect methylene in certain regions of dense interstellar clouds known as “hot cores” (12). The work of Lovas et al. (11) was followed by studies in the submillimetre-wave region by Ozeki and Saito (13), who measured the  $N_{K_a K_c} = 2_{12} \leftarrow 3_{03}$  and  $N_{K_a K_c} = 5_{05} \leftarrow 4_{14}$  multiplets of *para*-CH<sub>2</sub> at frequencies around 440–445 GHz and 592–594 GHz, respectively. Most recently, we studied the  $N_{K_a K_c} = 1_{11} \leftarrow 2_{02}$  rotational transition of *ortho*-CH<sub>2</sub> in the 931–956 GHz range, inaugurating the study of its THz spectrum at high resolution (14). A global data set consisting of all of the high-resolution spectral transitions was fit to an asymmetric top, Watson-type Hamiltonian with additional fine-structure and hyperfine-structure terms.

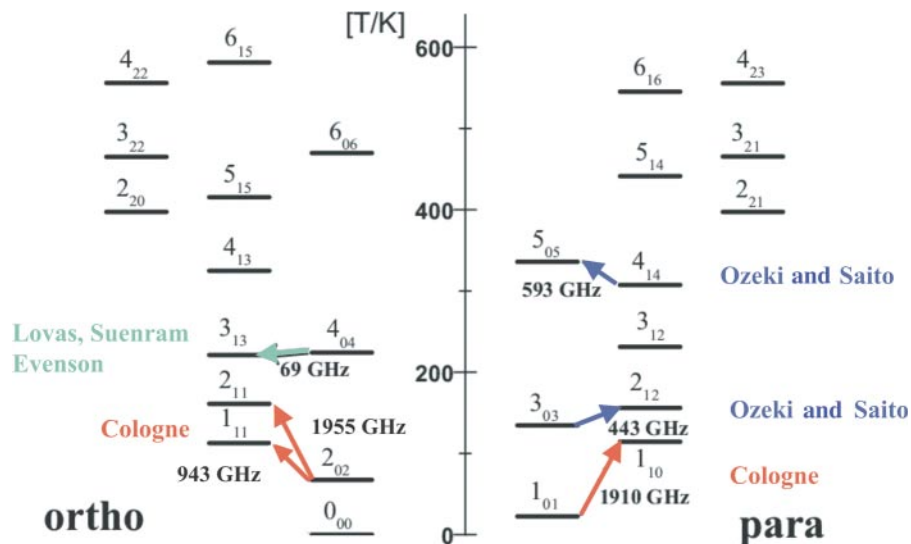
In this paper, we report the measurement of two new rotational transitions of the methylene radical in its ground vibrational-electronic state at frequencies near 2 THz. One of the transitions — the  $N_{K_a K_c} = 2_{11} \leftarrow 2_{02}$  multiplet of *ortho*-CH<sub>2</sub> — is centered at 1.954 GHz and consists of 23 detected components split by fine-structure and hyperfine effects. The other rotational transition is the  $N_{K_a K_c} = 1_{10} \leftarrow 1_{01}$  multiplet of *para*-CH<sub>2</sub>, which is split by fine-structure only, and is centered at 1.915 THz. Figure 1 shows the lowest lying rotational levels of methylene divided into *ortho* levels on the left and *para* levels on the right. Rotational transitions measured in the laboratory (including the present measurements) are depicted with arrows. The energy scale is in units of K, a convention favored by astronomers.

The remainder of this paper is divided as follows. First, we discuss the techniques used in the experimental measurements and show some of our spectral results. Then, we discuss the spectral assignments at 2 THz and our progress in fitting a global data set including the newly measured transitions to a standard Watson-type Hamiltonian with additional terms for fine-structure and hyperfine interactions. Progress has so far been partial only, and attempts with a nonrigid bender Hamiltonian will also be undertaken (6, 15). Afterwards, we discuss the role of methylene as an interstellar molecule. A discussion of current progress ends the paper.

## Experimental measurements

For the reported measurements, the Cologne sideband spectrometer for Terahertz applications (COSSTA) was used. A detailed description of the experimental setup to generate frequencies in the range from 1.75 to 2.01 THz is given by Gendriesch et al. (16). Here we only give a short summary of the techniques employed. The basic idea of a sideband system is to mix the outputs of two sources of radiation by means of a nonlinear device such as a fast Schottky diode, and filter out the generated sum frequency, known as the upper sideband, for spectroscopy. In our laser sideband system, one radiation source is a frequency stabilized FIR laser operated at a fixed frequency. The second frequency source is a

**Fig. 1.** Rotational levels of *ortho*- and *para*-methylene through an energy of 600 K ( $1 \text{ K} = 1.99 \times 10^{-3} \text{ kcal mol}^{-1}$ ). Measured transitions to microwave accuracy are indicated by arrows with names of groups.



backward wave oscillator (BWO) with a tunable frequency output that is phase, and therefore, frequency stabilized (17).

A sketch of the experimental setup, found in Fig. 2, is divided into four parts: (i) the phase-locked BWO unit with its frequency synthesizers (left), (ii) the sideband mixer inside the evacuated optics box (center), (iii) the optically pumped difluoromethane FIR laser system (lower right), and (iv) the cooled discharge cell with the major components necessary for efficient methylene production (upper right). The laser system is stabilized to the 15th harmonic of a 108 GHz Gunn oscillator followed by a THz quasi-optical harmonic mixer. The resulting IF is processed with an analog frequency demodulator to derive a sensitive control signal for the CO<sub>2</sub> laser stabilization, and hence for the FIR laser.

Sideband radiation is generated by mixing the output radiation of a phase-stabilized BWO with frequency-stabilized radiation of the FIR ring laser on a whisker-contacted, low-capacitance Schottky diode. The FIR laser system operates at a fixed frequency of 1.626 THz. Since the BWOs used can be continuously tuned within a frequency range from ~130 to 390 GHz, the produced upper sideband radiation (at a frequency given by the sum of BWO and FIR-laser frequency) covers a frequency region from 1.75 to 2.01 THz. The frequency stability of the whole system is determined by the loop error of the AFC (automatic frequency control). The error was measured to be less than 5 kHz.

The CH<sub>2</sub> was generated in two steps. First, commercially available diketene was pyrolyzed through quartz wool at 650 °C over a length of 20 cm to form ketene. The pure ketene was then discharged in a DC glow discharge at 40 mA and 50–80 μbar (1 bar = 100 kPa). The active region was ~80 cm with a cell diameter of 10 cm and could be cooled down to 170 K by a LN<sub>2</sub>-flowing copper jacket.

As in our previous work (14), fast square-wave Zeeman modulation was used to detect the CH<sub>2</sub> lines; the technique was adapted for the first time with the Cologne sideband spectrometer. For this purpose, a copper wire coil, able to withstand 30 A current, was attached surrounding the glass cell over the whole discharge length. An axial magnetic field

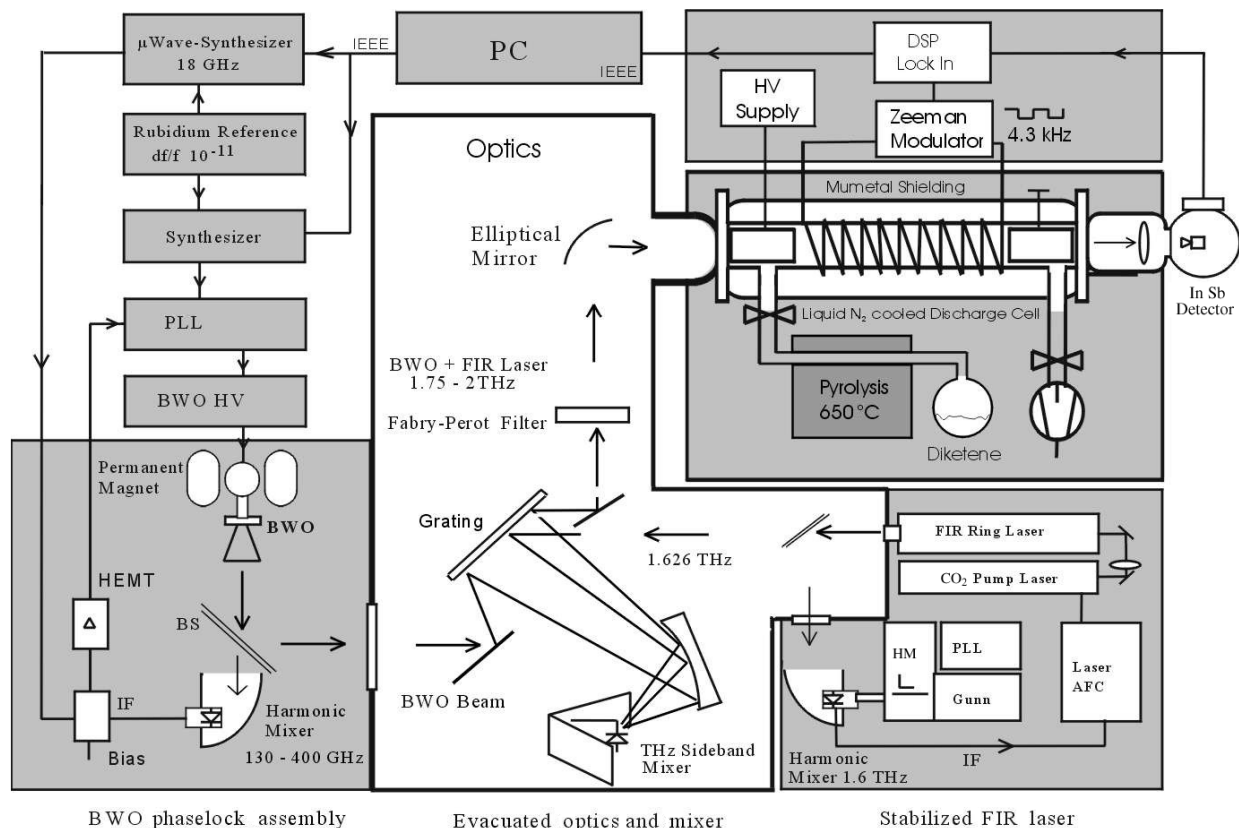
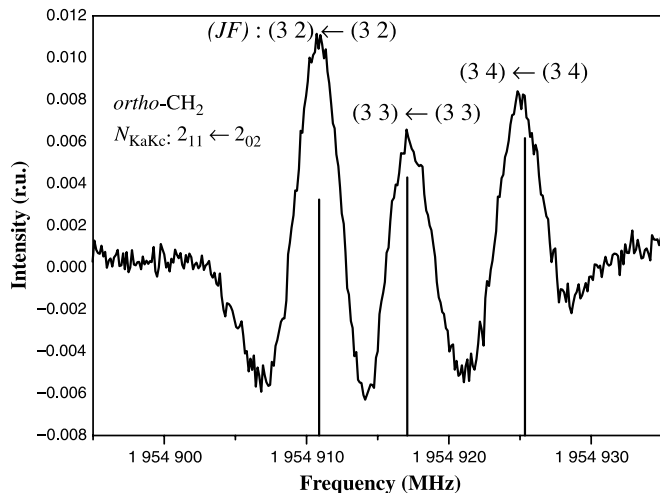
with  $B_{\text{max}} = 2$  to 3 G and a modulation frequency of 4.3 kHz could then be applied.

To shield the background earth magnetic field of 300–500 mG, a box of high permeable mu-metal (1mm thick) was constructed to cover the entire discharge region of the absorption cell. The residual magnetic field was measured to be below 10 mG. Special attention was paid to minimize induced eddy currents inside the shielding box that arise from the Zeeman modulation and may cause field inhomogeneities.

Table 1 contains the measured frequencies of the newly studied lines in MHz along with their quantum assignments and the uncertainties (one standard deviation) in the measured frequencies. Assignments with asterisks next to them are to be regarded as doubtful. The measurement uncertainties are typically 200 kHz for the components of the  $1_{10}$ – $1_{01}$  transition of *para*-CH<sub>2</sub> and 200–500 kHz for the corresponding components of the  $2_{11}$ – $2_{02}$  transition of *ortho*-CH<sub>2</sub>. The largest uncertainties arise from the weakness of some transitions and the overlapping of lines. These transitions were nonetheless included since the available rotational data for methylene are so sparse. Figure 3 shows the actual measured hyperfine structure for the  $J = 3 \leftarrow 3$  fine-structure component of the  $2_{11}$ – $2_{02}$  transition in the region 1954.910–1954.930 GHz, while Fig. 4 shows a stick spectrum with the complete fine-structure, hyperfine pattern for this rotational transition, which occurs over a much wider region between 1943 and 1964 GHz. Note that the assorted hyperfine-structure multiplets are designated by the letter *G* and an appropriate subscript. Figure 5 shows both the  $J = 2 \leftarrow 2$  and  $1 \leftarrow 0$  fine-structure components of the  $1_{10}$ – $1_{01}$  transition, split by more than 8 GHz, while Fig. 6 shows both the actual  $J = 2 \leftarrow 2$  component and a stick spectrum of all of the fine-structure components that extend over the region between 1902 and 1926 GHz.

## Spectral analysis

In our previous work on methylene, it was possible to uti-

**Fig. 2.** Scheme of Cologne sideband spectrometer for Terahertz applications (COSSTA). See text for detailed description.**Fig. 3.** Three newly measured spectral lines corresponding to the multiplet  $J = 3 \leftarrow 3$  ( $G_4$ ) of the rotational transition  $2_{11} \leftarrow 2_{02}$  of *ortho*-CH<sub>2</sub> and split by hyperfine interactions.

lize a Watson-type Hamiltonian plus assorted fine-structure and hyperfine-structure terms to fit the then global rotational spectrum to experimental accuracy (14). A total of 23 lines were fit to a Hamiltonian with 15 variable parameters and seven parameters held fixed at values derived by previous authors. As can be seen, there is an unusually large number of parameters needed compared with the number of lines, a common problem for other small, light asymmetric tops such as water.

The previous fit to the spectrum of methylene (14) based on the augmented Watson Hamiltonian was used to predict the frequencies of the components for the two rotational transitions studied here to perhaps 10 MHz accuracy. A similar degree of accuracy comes from the predictions based on the LMR work of Sears et al. (8). The Hamiltonian  $H$  can be written as:

$$[1] \quad H = H_{\text{rot}} + H_{\text{spin-spin}} + H_{\text{spin-rot}} + H_{\text{hfs}}$$

where the first term consists of the rigid-body and centrifugal distortion contributions (18), the second and third terms comprise the fine-structure interactions, and the last term represents the hyperfine contribution. For a light and floppy species such as CH<sub>2</sub>, the centrifugal distortion is appreciably large and cannot be neglected. The fine-structure terms arise from the electron spin-spin interaction, and the interaction of the electron spin with the rigid-body rotation of the molecule. As with the fine structure, there are two contributions to the hyperfine term, both of which have to do with the interaction among the electronic and nuclear spins. One term represents the so-called Fermi-contact interaction, while the second represents the dipole-dipole interaction. Matrix elements were derived for the Hamiltonian in the coupling scheme  $\mathbf{J} = \mathbf{N} + \mathbf{S}$ ,  $\mathbf{F} = \mathbf{J} + \mathbf{I}_H$ ,  $\mathbf{I}_H = \mathbf{I}_{H(1)} + \mathbf{I}_{H(2)}$ . More detail on the various terms in the Hamiltonian and the procedure used to fit and predict the spectrum can be found in our previous publication (14).

A global data set comprising the previously measured transitions and those reported here was fit to the Hamiltonian discussed above. Based on this information, Figs. 7 and

**Table 1.** Newly measured spectral lines of CH<sub>2</sub> in its ground electronic–vibrational state.

$J',F'-J'',F''$	$\nu_{\text{obs}}$ (MHz) <sup>a</sup>
$1_{10}-1_{01}$	
1-1	1 902 654.362(200)
2-1	1 907 986.637(300)
1-2	1 912 328.935(200)
0-1	1 916 348.190(200)
2-2	1 917 661.094(100)
1-0	1 925 866.221(200)
$2_{11}-2_{02}$	
1,1-2,2	1 942 878.947(300)*
1,2-2,3	1 942 910.487(300)
3,4-2,3	1 944 411.017(300)
3,3-2,2	1 944 448.270(300)
3,2-2,1	1 944 476.330(500)
2,3-2,3	1 949 051.376(500)*
2,2-2,2	1 949 058.720(500)*
2,1-2,1	1 949 063.340(500)*
3,2-3,2	1 954 910.784(500)
3,3-3,3	1 954 917.270(500)
3,4-3,4	1 954 925.038(500)
3,2-3,3	1 954 943.129(500)*
3,3-3,4	1 954 959.111(500)*
1,1-1,2	1 958 077.452(500)
1,2-1,2	1 958 112.867(300)
1,0-1,1	1 958 112.867(300)*
1,1-1,1	1 958 130.100(500)*
1,1-1,0	1 958 156.446(500)
1,2-1,1	1 958 165.435(500)
2,1-3,2	1 959 496.844(300)
2,2-3,3	1 959 526.242(300)
2,3-3,4	1 959 564.919(200)
2,3-1,2	1 964 253.432(500)

**Note:** The asterisks represent lines for which the assignment is ambiguous.

<sup>a</sup>The numbers in parentheses represent experimental uncertainties (one standard deviation) in terms of the right-most significant figures.

8 summarize how the rotational levels for the  $1_{10}-1_{01}$  transition are split and shifted by fine-structure interactions and for the  $2_{11}-2_{02}$  transition by both fine- and hyperfine-structure interactions. Although the qualitative aspects of the figures are certainly correct, the detailed numbers must be taken with caution since they may not be accurate to the 1 MHz level depicted. The current status of the fit *as it pertains to the newly measured transitions* is that the individual components show observed – calculated deviations from a low of 0.1 MHz to a high of 8 MHz, the latter far greater than the experimental uncertainty. For the fine-structure components of the  $1_{10}-1_{01}$  transition of *para*-CH<sub>2</sub>, the separation is sufficiently great that the assignments are unambiguous. But, for the  $2_{11}-2_{02}$  transition of *ortho*-CH<sub>2</sub>, the hyperfine components of each group  $G_i$  of lines can lie sufficiently close together so as to leave the assignment ambiguous. For such lines, Table 1 contains an asterisk next to the measured frequency. Currently, eight out of the 23 measured components of this rotational transition lie in this category.

## Interstellar importance

Almost four decades after its original detection in the laboratory, CH<sub>2</sub> was finally detected in emission in the interstellar medium by Hollis et al. (12), based on the *ortho*-CH<sub>2</sub> rotational transition  $N_{\text{KaKc}} = 4_{04} \leftarrow 3_{13}$  at 68–71 GHz, previously studied in the laboratory in absorption by Lovas et al. (11). As can be seen in Fig. 1, the upper level of this rotational transition lies at an excitation of approximately 240 K, which means that for collisional excitation to populate it appreciably, the temperature of the medium has to be comparable. Dense interstellar clouds are mainly colder than this, with kinetic temperatures in the region 10–50 K, but exceptions are found in regions associated with star formation. When high-mass stars are formed, there is enough energy to heat surrounding regions to 300 K and even beyond. It is in two such regions, labelled hot cores by astronomers, that Hollis et al. found methylene.

According to chemical models of interstellar gas (19), however, the methylene radical should be an ubiquitous tracer of colder interstellar gas. To detect CH<sub>2</sub> in colder gas requires lower-lying upper states, which tend, however, to be associated with transitions that possess frequencies in the THz region of the spectrum. For example, the lowest-lying emitting level of *ortho*-CH<sub>2</sub> is the  $1_{11}$  level, which lies at little over 100 K above the ground. This level can emit to either the  $2_{02}$  level, at frequencies around 943 GHz, measured by us previously (13), or to the ground  $0_{00}$  level, at frequencies around 2345 GHz (8). For *para*-CH<sub>2</sub>, the lowest emitting level is the  $1_{10}$  level, which also lies at an excitation of little more than 100 K. This level can emit to the ground state of *para*-CH<sub>2</sub> at the frequencies reported here, in the vicinity of 1910 GHz.

Transitions that occur at frequencies in the submillimeter-wave region cannot easily be measured from the ground because of the water vapor in the atmosphere of the earth. Although some ground-based facilities do exist for which strong transitions can be measured up to frequencies near 1 THz, the THz region is essentially inaccessible from the ground. For this and other reasons, astronomers have launched satellites and flown high-elevation airplanes to detect submillimeter-wave and shorter radiation from high up or above the atmosphere. Two future missions will be suited to study spectral transitions in the THz region. The project named SOFIA (<http://sofia.arc.nasa.gov>) will contain a telescope in a Boeing 747-SP aircraft and will have a high-resolution spectrometer in the region between 500 GHz and 4 THz. An even more sensitive telescope, named Herschel, is to be placed in orbit around the so-called L2 point of the earth–sun system (<http://herschel.jpl.nasa.gov>). The high-resolution THz spectrometer for Herschel, named HIFI, will operate in several bands through 1910 GHz. Detection of methylene with either of these telescopes should be achievable in cold regions of the interstellar medium if the current predictions of chemical models are accurate.

## Discussion

We have chosen in part to study the molecular radical CH<sub>2</sub> because it played an important role in Gerhard Herzberg's scientific life. In addition, CH<sub>2</sub> appears to be one of the sim-

**Fig. 4.** A stick spectrum showing the frequencies and relative intensities of all lines of the rotational transition  $2_{11} \leftarrow 2_{02}$  of *ortho*-CH<sub>2</sub>. Each group of lines designed by  $G_i$  ( $i = 1-7$ ) represents components belonging to a common fine-structure transition ( $N', J' \leftarrow N'', J''$ ) but split by hyperfine effects. Asterisks indicate measured and assigned lines.

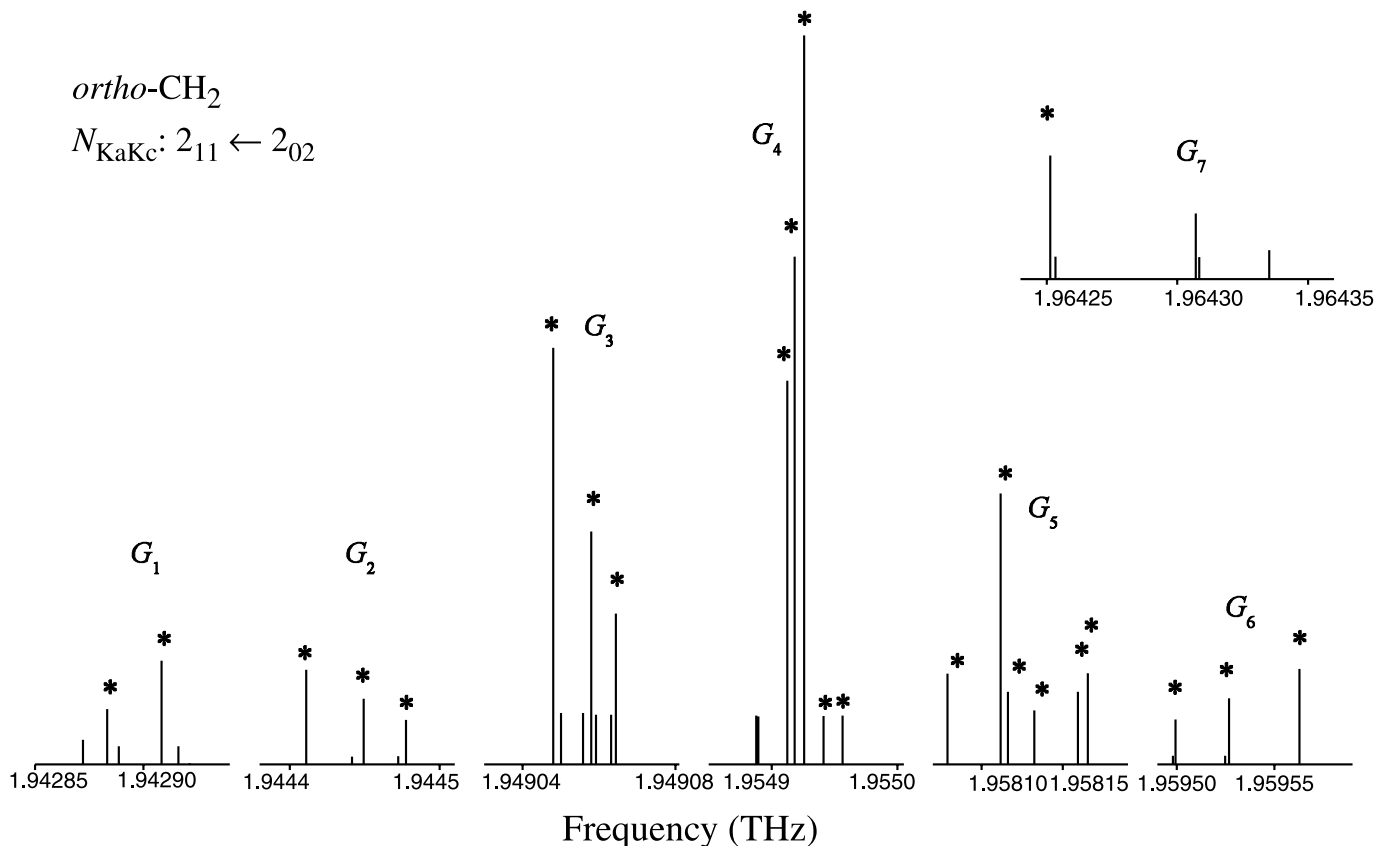
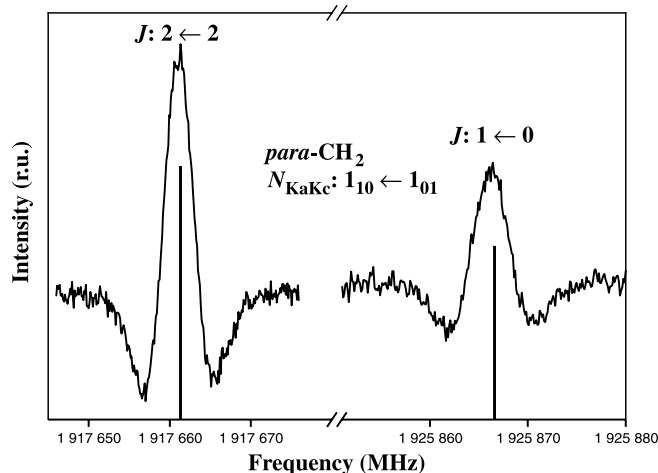
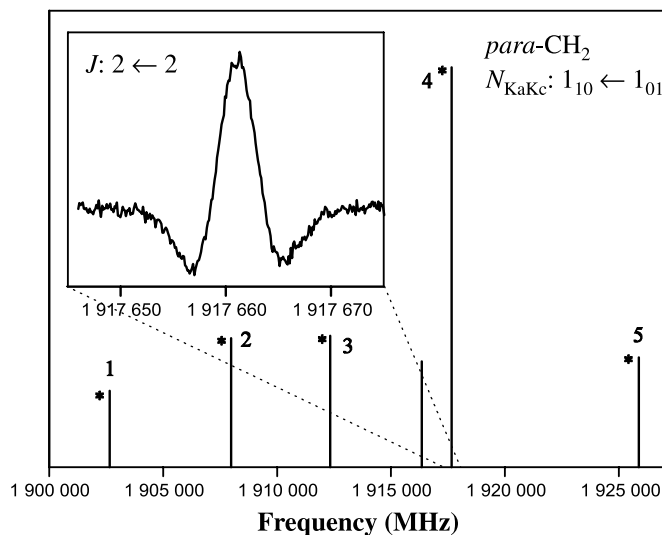


**Fig. 5.** Two newly measured fine-structure components of the  $1_{10} \leftarrow 1_{01}$  rotational transition of *para*-CH<sub>2</sub>. The sticks represent calculated frequencies and relative intensities.



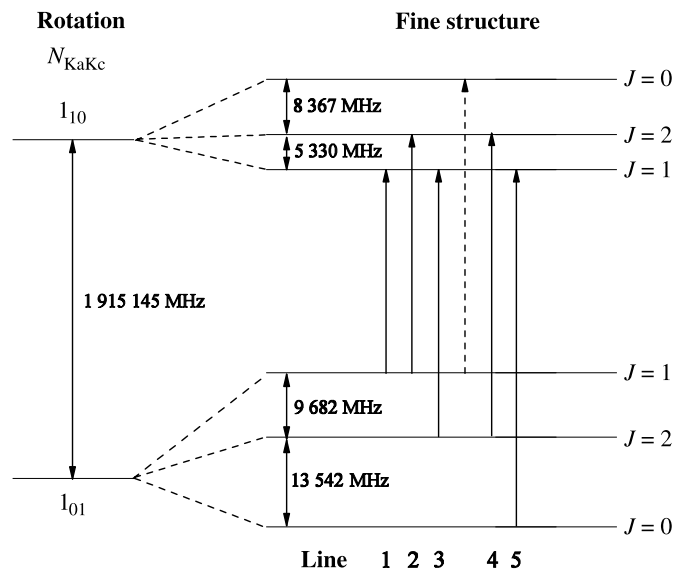
plest free radicals in chemistry. But, the laboratory spectrum of CH<sub>2</sub> has proven difficult to study in all wavelength regions for a variety of reasons, including its lightness, and its intricate fine and hyperfine structure. For its rotational spectrum, CH<sub>2</sub> displays a perpendicular *b*-type spectrum, which is proving to be one of the most difficult to understand. One reason for the difficulty is the fact that the rotational spec-

**Fig. 6.** A stick spectrum showing the frequencies and relative intensities of the six fine-structure components of the  $1_{10} \leftarrow 1_{01}$  rotational transition of *para*-CH<sub>2</sub>. All lines shown are measured and assigned. The actual measured spectral line designated by the number 4 (the  $J = 2 \leftarrow 2$  component) is also shown.



trum is not confined to the rather standard microwave region, but ranges through the THz region into the far-IR! Perhaps the dominant reason for the difficulty is the fact that

**Fig. 7.** Energy level diagram of the  $1_{10}$ – $1_{01}$  rotational transition of *para*-CH<sub>2</sub>. The splitting of the rotational levels by fine-structure interactions is shown. The six allowed rotational-fine structure transitions, all of which have been measured, are also shown. Actual numbers shown are uncertain due to the incomplete nature of the fit to the data.

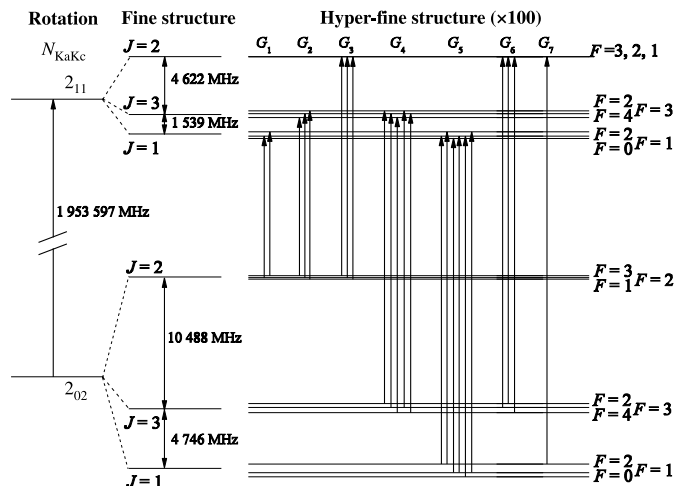


the molecule undergoes large amplitude motion so that the coordinates of the two hydrogen atoms and the carbon atom are not strictly defined. Indeed, the potential function along the appropriate coordinates is very shallow and fairly flat near the equilibrium position, lending the three atoms a restricted freedom to move around their equilibrium positions.

In the problem of large amplitude motions, methylene is not unique. The spectroscopic properties of other light asymmetric rotors such as H<sub>2</sub>O, H<sub>2</sub>S, NH<sub>2</sub> ( $X^2B_1$ ), and PH<sub>2</sub> ( $X^2B_1$ ), have been analyzed, in some cases with extreme difficulty, with the aid of the Watson Hamiltonian for asymmetric rotors (20–22). All of these triatomic molecules display large amplitude motions to various degrees, producing convergence problems of the angular momentum power representation for the Hamiltonian. For light molecules, higher order effects become appreciably large even at low rotational quantum numbers, because the rotational energies are already high. One is therefore forced to include into the rotational Hamiltonian high-order centrifugal distortion terms.

In this paper, we have reported our current state of progress on measuring, assigning, and fitting the pure rotational spectrum of the methylene radical (CH<sub>2</sub>). Although we were able to fit a small number of fine- and hyperfine-split components of several rotational transitions in a previous investigation (14), addition of the newly measured lines reported here appears to exacerbate previous difficulties in fitting the global spectrum to a standard Watson-type effective Hamiltonian. At present, we can fit most of the newly measured lines that belong to the  $1_{10}$ – $1_{01}$  rotational transition of *para*-CH<sub>2</sub> at 1902–1926 GHz, and the  $2_{11}$ – $2_{02}$  rotational transition of *ortho*-CH<sub>2</sub> at 1943–1964 GHz, as part of a global fit to an accuracy good enough for assignment purposes. A significant minority of lines, however, especially those lying in closely spaced multiplets split by hyperfine ef-

**Fig. 8.** Energy level diagram of the  $2_{11}$ – $2_{02}$  rotational transition of *ortho*-CH<sub>2</sub>. The splitting of the rotational levels by fine-structure and hyperfine interactions is depicted. The 23 measured components, divided into seven groups designated by  $G_i$  ( $i = 1$ – $7$ ) are also indicated. Actual numbers shown are uncertain due to the incomplete nature of the fit to the data.



fects, cannot be unambiguously assigned. Nor is the average deviation between the newly observed and calculated frequencies anywhere near experimental measurement accuracy. Indeed, some lines have observed–calculated frequencies as large as 8 MHz. The rotational, fine structure, and hyperfine structure constants obtained from fits that include our new data at 2 THz are distinctly not improved over our previous values (14).

To better our understanding of the spectrum, we are currently trying two alternative approaches to conventional spectroscopy. The first is the use of the Morse oscillator-rigid bender internal dynamics (MORBID) Hamiltonian (6, 15) to determine the rotational energy levels in place of the standard Watson-type Hamiltonian. The second is an Euler expansion of the rotational parameters to constrain the rotational structure, an approach that works nicely for water (23).

The MORBID approach is different from the Watsonian-type treatment of rotation–vibration states in that it provides an, in principle complete, solution of the rotation–vibration Schrödinger equation for the electronic state in question. Thus, it is possible to calculate the energies of a large number of rotation–vibration energies directly from the potential energy surface, which is represented by a parameterized analytical function, the parameter values of which are the input data for the calculation of this electronic state. Also, the potential energy parameters can be refined in fittings to experimental rotation–vibration data, as done by Jensen and Bunker (6), who used all extant rotation–vibration data for  $\tilde{X}^3B_1$  CH<sub>2</sub>. MORBID is based on a theory first proposed by Hougen et al. (24) and designed so that it is applicable to both linear and bent triatomic molecules. Therefore, it describes well, for example, the dramatic change of the *A* rotational constant resulting from excitation of the bending vibration in the  $\tilde{X}$ -state of CH<sub>2</sub>. Since *all* rotation–vibration energies of the electronic state are determined in terms of a rather small number of potential energy parameters (which

are the only parameters that can be adjusted in least-squares fittings to experimental data), the residuals observed in the fittings are generally larger by orders of magnitude than those obtained in fittings with Watsonian models. However, because of the shortcomings of the Watsonian model for light molecules with highly anharmonic potential energy surfaces, such as  $\tilde{X}^3 B_1 CH_2$ , the predictive power of MORBID is sometimes better than that of the Watsonian model.

Gerhard Herzberg said in his Nobel lecture "... of course the spectrum of  $CH_2$  has given me a great deal of pleasure..." (4). His first attempts to savour it date back to 1942, and the story of its discovery is long, difficult, slow, and not yet finished. Now, more than 60 years later and despite much progress, the  $CH_2$  problem remains with us.

### Acknowledgments

GW thanks the Deutsche Forschungsgemeinschaft for its support via special grant SFB-494. He also thanks the Ministry of Science of the Land Nordrhein-Westfalen for special funding. EH wishes to acknowledge NASA for its support of the Ohio State program in laboratory astrophysics.

### References

1. B. Stoicheff. *Gerhard Herzberg: An Illustrious Life in Science*. NRC Research Press, Ottawa. 2002.
2. G. Herzberg and J. Shoosmith. *Nature (London)*, **183**, 1801 (1959).
3. G. Herzberg and J.W.C. Johns. *J. Chem. Phys.* **54**, 2276 (1971).
4. G. Herzberg. *Nobel Lectures in Chemistry 1971–1980. Edited by S. Forsen*. World Scientific, Singapore. 1993. pp. 9–46.
5. M.D. Marshall and A.R.W. McKellar. *J. Chem. Phys.* **85**, 3716 (1986).
6. P. Jensen and P.R. Bunker. *J. Chem. Phys.* **89**, 1327 (1988).
7. T.J. Sears, P.R. Bunker, A.R.W. McKellar, K.M. Evenson, D.A. Jennings, and J.M. Brown. *J. Chem. Phys.* **77**, 5348 (1982).
8. T.J. Sears, A.R.W. McKellar, P.R. Bunker, K.M. Evenson, and J.M. Brown. *Astrophys. J.* **276**, 399 (1984).
9. T.J. Sears. *J. Chem. Phys.* **85**, 3711 (1986).
10. P.R. Bunker and S.R. Langhoff. *J. Mol. Spectrosc.* **102**, 204 (1983).
11. F.J. Lovas, R.D. Suenram, and K.M. Evenson. *Astrophys. J.* **267**, L131 (1983).
12. J.M. Hollis, P.R. Jewell, and F.J. Lovas. *Astrophys. J.* **438**, 259 (1995).
13. H. Ozeki and S. Saito. *Astrophys. J.* **451**, L97 (1995).
14. E.A. Michael, F. Lewen, G. Winnewisser, H. Ozeki, H. Habara, and E. Herbst. *Astrophys. J.* **596**, 1356 (2003).
15. P. Jensen. *J. Mol. Spectrosc.* **128**, 478 (1988).
16. R. Gendriesch, F. Lewen, G. Winnewisser, and J. Hahn. *J. Mol. Spectrosc.* **203**, 205 (2000).
17. F. Lewen, R. Gendriesch, I. Pak, D.G. Paveliev, M. Hepp, R. Schieder, and G. Winnewisser. *Rev. Sci. Instrum.* **69**, 32 (1998).
18. W. Gordy and R.L. Cook. *Microwave molecular spectroscopy*. Wiley, New York. 1984.
19. H.H. Lee, R.P.A. Bettens, and E. Herbst. *Astron. Astrophys. Suppl. Ser.* **119**, 111 (1996).
20. A.H. Saleck, M. Tanimoto, S.P. Belov, T. Klaus, and G. Winnewisser. *J. Mol. Spectrosc.* **171**, 481 (1995).
21. R. Gendriesch, F. Lewen, G. Winnewisser, and H.S.P. Müller. *J. Mol. Struct.* **599**, 293 (2000).
22. L. Margulès, E. Herbst, V. Ahrens, F. Lewen, G. Winnewisser, and H.S.P. Müller. *J. Mol. Spectrosc.* **211**, 211 (2002).
23. H.M. Pickett and J.C. Pearson. *Ohio State Univ. Int. Symp. Mol. Spectrosc.* **57**, 108 (2001).
24. J.T. Hougen, P.R. Bunker, and J.W.C. Johns. *J. Mol. Spectrosc.* **34**, 136 (1970).